Jonathan L. Brisman, M.D.

Epilepsy Research Laboratory, and Neurosurgical Service, Massachusetts General Hospital, Harvard Medical School, Boston, Massachusetts

G. Rees Cosgrove, M.D.

Neurosurgical Service, and Northeast Proton Beam Regional Therapy Center, Massachusetts General Hospital, Harvard Medical School, Boston, Massachusetts

Allan F. Thornton, M.D.

Northeast Proton Beam Regional Therapy Center, and Department of Radiation Oncology, Massachusetts General Hospital, Harvard Medical School, Boston, Massachusetts

Thomas Beer, B.S.

Epilepsy Research Laboratory, Massachusetts General Hospital, Harvard Medical School, Boston, Massachusetts

Maria Bradley-Moore, A.B.

Epilepsy Research Laboratory, Massachusetts General Hospital, Harvard Medical School, Boston, Massachusetts

Christina T. Shay, A.B.

Epilepsy Research Laboratory, Massachusetts General Hospital, Harvard Medical School, Boston, Massachusetts

E. Tessa Hedley-Whyte, M.D.

Department of Neuropathology, Massachusetts General Hospital, Harvard Medical School, Boston, Massachusetts

Andrew J. Cole, M.D.

Epilepsy Research Laboratory, Massachusetts General Hospital, Harvard Medical School, Boston, Massachusetts

Reprint requests:
Jonathan L. Brisman, M.D., Institute for Neurology and Neurosurgery, Roosevelt Medical Center, 1000 Tenth Avenue, New York, NY 10019.

Received, April 12, 2004.
Accepted, December 2, 2004.

HYPERACUTE NEUROPATHOLOGICAL FINDINGS AFTER PROTON BEAM RADIOSURGERY OF THE RAT HIPPOCAMPUS

OBJECTIVE: To study the hyperacute histological and immunohistochemical effects of stereotactic proton beam irradiation of the rat hippocampus.

METHODS: Nine rats underwent proton beam radiosurgery of one hippocampus with nominal doses of cobalt-2, -12, and -60 Gray equivalents (n = 3 each). Control animals (n = 3) were not irradiated. Animals were killed 5 hours after irradiation and brain sections were stained for Nissl, silver degeneration, deoxyribonucleic acid (DNA) fragmentation (DNAF), and the activated form of two mitogen-activated protein kinases (MAPKs), phospho-Erk1/2 (P-Erk1/2) and p38. Stained cells in the hippocampus expressing DNAF and/or P-Erk1/2 were counted. Confocal microscopy with double immunofluorescent staining was used to examine cellular colocalization of DNAF and P-Erk1/2.

RESULTS: Both DNAF and P-Erk1/2 showed quantitative dose-dependent increases in staining in the targeted hippocampus compared with the contralateral side and controls. This finding was restricted to the subgranular proliferative zone of the hippocampus. Both markers also were up-regulated on the contralateral side when compared with controls in a dose-dependent fashion. Simultaneous staining for DNAF and P-Erk1/2 was found in fewer than half of all cells. p38 was unchanged compared with controls. Although Nissl staining appeared normal, silver stain confirmed dose-dependent cellular degeneration.

CONCLUSION: DNAF, a marker of cell death, was present in rat hippocampi within 5 hours of delivery of cobalt-2 Gray equivalents stereotactically focused irradiation, suggesting that even low-dose radiosurgery has hyperacute neurotoxic effects. Activated mitogen-activated protein kinase was incompletely colocalized with DNAF, suggesting that activation of this cascade is neither necessary nor sufficient to initiate acute cell death after irradiation.

KEY WORDS: Deoxyribonucleic acid fragmentation, Mitogen-activated protein kinase, Proton beam, Radiosurgery, Rat, Silver stain

Neurosurgery 56:1330-1338, 2005 DOI: 10.1227/01.NEU.0000159885.34134.20 www.neurosurgery-online.com

Stereotactic radiosurgery, used primarily to treat intracranial neoplasms and vascular malformations, is used as a neurosurgical tool with increasing frequency in the treatment of intractable temporal lobe epilepsy, trigeminal neuralgia, and movement disorders. This increased use and availability of stereotactic radiosurgery warrants an increased understanding of the basic radiobiology of radiosurgery.

The experimental literature delineating the effects of stereotactic irradiation on the brain has focused on the late effects of irradiation after a certain latency, typically after weeks or months. This time point frequently is chosen to mimic the response of the human brain to irradiation, where both therapeutic and untoward effects are usually not seen until months or even years after administration. Relatively little research has focused on the early, that is, acute (<1 wk) or hyperacute (<24 h), effects of radiosurgery, yet there is evidence that biochemical changes occur in mammalian brain early after radiosurgery, even at low doses. Histological and biochemical changes have been demonstrated acutely in rats after treatment with gamma knife to the forebrain (46), x-rays to the whole brain (1), and protons to

the right hemisphere (22), as well as hyperacutely in the rat brain after whole body mixed neutron-gamma irradiation (3, 32), whole brain gamma irradiation (15), whole brain x-rays (44), and linear accelerator radiosurgery irradiation (39). Both hyperacute and acute changes also have been studied in a systemic irradiation model in mice (35). More specifically, apoptotic, but not necrotic, cell death has been documented in the subependyma, corpus callosum, and subgranular proliferative zone (SGZ) of the dentate gyrus in the adult rat within a few hours after brain irradiation with doses as low as 0.5 Gy (1). Because changes that take place in the early period after irradiation may be responsible for effects seen months or years later, studying these early changes may shed light on findings at delayed time points.

We sought to better define the early effects of radiosurgery using a newly developed model of proton beam radiosurgery (PBR) of the rat hippocampus (4). We defined a dose-response curve using two stains for cell death (deoxyribonucleic acid [DNA] fragmentation [DNAF] and silver stain) and immunostains for the activated or phosphorylated form of the neuronal isoform of mitogen-activated protein kinase (MAPK), phospho-Erk1/2 (P-Erk1/2) or p38. MAPKs, which include Erk and p38, represent a family of intracellular enzymes activated by phosphorylation that transduce extracellular events into intracellular signals by triggering a cascade of phosphorylation and downstream signaling. The up-regulated form of MAPK has been shown to be a sensitive marker to various stressors, including irradiation, and there is some evidence that it may be linked to apoptotic cell death in some circumstances (5). We therefore used double-immunostaining confocal microscopy with DNA fragmentation and P-Erk1/2 to ask whether focused hippocampal radiation-induced cell death is correlated with activation of either of two MAPKs, P-Erk1/2 or p38.

MATERIALS AND METHODS

Animal Care

All experiments were conducted in accordance with the guidelines for animal care set forth by the Subcommittee for Research and Animal Care of Massachusetts General Hospital. Rats were housed on a 12-hour light-dark cycle and given free access to food and water. Metallic ear tags were used to track animal identity. All animals were male Sprague-Dawley descendant rats (250–350 g; Charles River Laboratories, Wilmington, MA).

Animal Radiosurgical Device/Stereotactic Radiosurgery

Proton beam delivery to the right hippocampus of the rat was carried out at the Harvard Cyclotron Laboratory using a specially designed stereotactic head frame and brass aperture. The details of stereotactic planning and dose delivery, including isodose curves and exact measurements of the target, have been described previously (4).

Tissue Preparation

Animals were anesthetized with pentobarbital (100 mg/kg) and perfusion fixed with 4% paraformaldehyde. After storage in situ overnight at 4°C, the brains were harvested, weighed, and cut on a sliding Vibratome (Vibratome Co., St. Louis, MO) in 0.1 mol/L phosphate buffer (50 μm).

Histological Analysis

Coronal sections were stained with 0.1% cresyl violet, cover-slipped, and examined by light microscopy. Silver staining for neuronal degeneration was performed using the technique of Gallyas et al. (18) as described by Nadler and Evenson (34). Silver-stained cells were counted manually in each tissue section. Cell counts were averaged for each animal. The average cell counts and standard deviations were calculated for the groups of animals at each dose.

Immunohistochemistry

For DNAF and P-Erk1/2 double immunostaining, free-floating brain tissue sections were treated according to the protocol of Weiss et al. (45) for terminal deoxynucleotidyl transferase-mediated nick end labeling (TUNEL) of fragmented DNA with biotin-21-deoxyuridine triphosphate (Clontech Laboratories, Inc., Palo Alto, CA). Sections were then incubated for 1 hour in 0.3% Triton solution and overnight at 4°C in 5% goat serum blocking buffer containing mouse monoclonal biotin antibody (1:50 dilution; Boehringer Mannheim, Indianapolis, IN) and rabbit polyclonal phospho-p44/42 MAP kinase antibody (1:50 dilution; New England Biolabs, Beverly, MA). The following day, sections were incubated for 1 hour in 5% goat serum-blocking buffer containing BODIPY-conjugated goat anti-mouse antibody (1:50 dilution; Molecular Probes, Eugene, OR) and Cy3-conjugated goat antirabbit antibody (1:200 dilution; Jackson ImmunoResearch Laboratories, Inc., West Grove, PA). Finally, sections were mounted on slides and cover-slipped using Aqua Poly/Mount (Polysciences, Inc., Warrington, PA).

Fluorescent-labeled tissue sections were viewed at $\times$200 magnification with a confocal microscope and Lasersharp software (Bio-Rad, Hercules, CA). Digital images were taken of the dentate gyrus of both hippocampi in brain sections from each animal. Cy3-labeled P-Erk1/2 was recorded in the red channel, whereas BODIPY-labeled TUNEL staining for DNAF was recorded in the green channel, and a composite image was recorded in a third channel for analysis with PhotoShop 5.5 software (Adobe Systems, Mountain View, CA). For each image, cell counts were made of MAPK-labeled, TUNEL-labeled, and double-labeled cells in the SGZ and the dentate granule cell layer. Cell counts were averaged for each animal. Average cell counts and standard deviations for groups of animals at each dose were calculated.

For p38 detection, free-floating sections were washed in phosphate-buffered saline (PBS) for 10 minutes (three times) and for 1 hour in 0.3% Triton X-100 in a blocking buffer consisting of 5% normal goat serum in PBS. Sections then were

incubated overnight at 4°C in polyclonal rabbit antibody for phosphorylated p38 MAPK (New England Biolabs) diluted 1:500 in blocking buffer. The following day, sections were washed for 10 minutes (six times) in PBS and were incubated overnight at 4°C in biotinylated goat anti-rabbit antibody (Vector Laboratories, Burlingame, CA) diluted 1:200 in blocking buffer. On the third day, sections were washed for 10 minutes (six times) in PBS, then for 30 minutes in 0.3% hydrogen peroxide in PBS. Next, sections were incubated for 1 hour in ABC (Vectastain Elite; Vector Laboratories) and were washed again for 10 minutes in PBS. Immunoreactivity was visualized with diaminobenzidine tetrachloride as the chromogen. Finally, the sections were mounted on slides, coverslipped with Permount (Fisher Scientific, Pittsburgh, PA), and examined using a light microscope.

Statistical Analysis

A mixed linear model was used to compare the difference between the targeted hippocampus and the contralateral side across doses, the difference between targeted sides across doses, and the difference between the nontargeted sides across doses for DNAF, P-Erk1/2, and silver stain. The percentage of colocalization of DNAF and P-Erk1/2 was assessed using the same dosage groups. A statistical correlation test determined whether the score for double-stained cells (calculated as the total number of cells, T, divided by the product of the total number of DNAF stained cells, D, and the total number of P-Erk1/2-stained cells, E, for a given hippocampus) correlated with dose, Q. P values <0.05 were considered statistically significant.

RESULTS

DNAF and P-Erk1/2

DNAF and P-Erk1/2 both showed a dose-dependent increase in staining in targeted hippocampi compared with nontargeted hippocampi and controls (*Figs. 1–3*; *Table 1*). Two cobalt Gray equivalents (CGEs) did not induce staining for either DNAF or P-Erk1/2 when the targeted side was compared with controls. The contralateral (nontargeted) hippocampi showed marked P-Erk1/2 up-regulation and DNAF staining when compared with controls after cobalt-60 Gray equivalent (60 CGE) only ($P \leq 0.001$ and $P \leq 0.005$, respectively). Staining within the hippocampus was restricted to the SGZ (*Figs. 1, 2*; *Table 1*).

Comparisons also were made between targeted and nontargeted hippocampi for different doses of irradiation. For P-Erk1/2, significantly more staining was detected in the targeted hippocampus compared with the contralateral hippocampus of cobalt-12 Gray equivalent (12 CGE) animals when compared with the cobalt-2 Gray equivalent (2 CGE) or 60 CGE group ($P \leq 0.001$). When comparing the targeted with the nontargeted sides, 2 CGE was enough to induce significant DNAF staining (*Table 1*). P-Erk1/2 also showed significantly increased staining on the targeted side compared with the contralateral side with 60 CGE and 12 CGE when compared with hippocampi targeted with only 2 CGE ($P \leq 0.001$). Interestingly, for both DNAF and P-Erk1/2, staining of the targeted hippocampus compared with the contralateral side was slightly more impressive at 12 CGE ($P \leq 0.001$) than at 60 CGE ($P = 0.0038$) (*Figs. 1, 2*; *Table 1*).

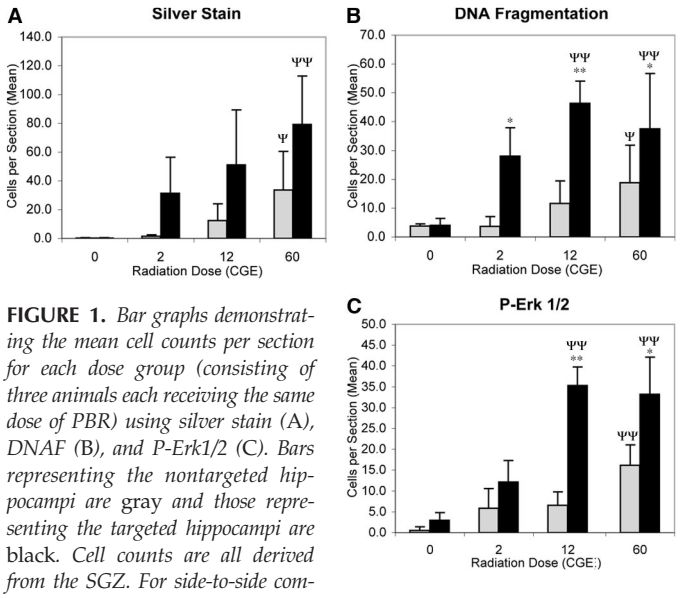

FIGURE 1. *Bar graphs demonstrating the mean cell counts per section for each dose group (consisting of three animals each receiving the same dose of PBR) using silver stain (A), DNAF (B), and P-Erk1/2 (C). Bars representing the nontargeted hippocampi are* gray *and those representing the targeted hippocampi are* black. *Cell counts are all derived from the SGZ. For side-to-side comparisons within a group: *, $P \leq 0.05$ and **, $P \leq 0.001$. For within-side comparisons to control group (0 CGE, nonirradiated): Ψ, $P \leq 0.05$ and ΨΨ, $P \leq 0.001$. Comparisons between irradiated groups are not depicted. Note: ordinate scales differ between graphs.*

Silver Stain

Staining for silver degeneration revealed significant increased staining at the highest dose (60 CGE) only. This finding also was restricted to the SGZ and was significant on both the targeted ($P = 0.003$) and contralateral side ($P = 0.0006$) when compared with controls. Interestingly, there was no significant difference between the targeted hippocampus and the contralateral hippocampus in comparison with the difference seen in the controls at each dose used. Intergroup comparisons of irradiated animals was significant only for an increased staining of 60 CGE when compared with 2 CGE on the nontargeted side ($P = 0.001$). Although qualitative light microscopic analysis suggested that at both 2 CGE and 12 CGE there was a significant increase in silver staining between irradiated hippocampi and nonirradiated control hippocampi, this was not borne out by statistical analysis (*Fig. 3*; *Table 1*).

DNAF and P-Erk1/2 Double Staining

Percentage of double-stained cells ranged from 22 to 42% on the targeted side compared with 27 to 30% on the nonirradiated side (*Fig. 4*; *Table 1*). Although there was no correlation between different doses and percent double staining, there was a strong positive correlation between number of double-

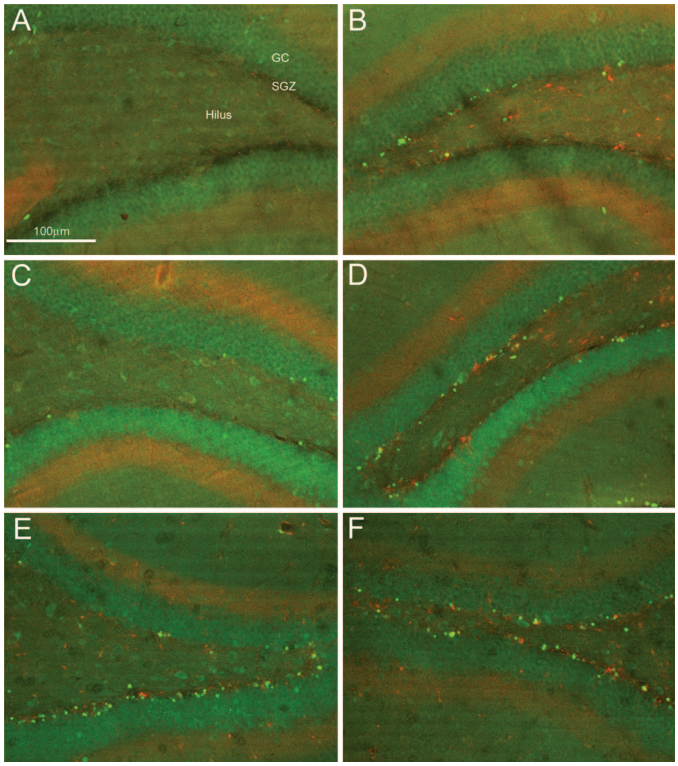

FIGURE 2. *Confocal microscopic images of rat hippocampal dentate gyrus after double immunofluorescent staining for DNAF* (green) *and P-Erk1/2* (orange) *using varying doses of PBR. Nontargeted* (A, C, *and* E; *original magnification, ×50) and targeted sides* (B, D, *and* F; *original magnification, ×50) of hippocampi that had received 2 CGE* (A *and* B), *12 CGE* (C *and* D), *or 60 CGE* (E *and* F) *are shown. The dose dependency for both stains is best appreciated as one views the progression of staining on the nontargeted sides* (A, C, *and* E) *with incremental dosing, most likely the result of irradiation scatter.* GC, *granule cell layer;* SGZ, *subgranular proliferative zone.*

stained cells in hippocampi of animals receiving irradiation (any dosage) as compared with nontargeted hippocampi (Spearman correlation coefficient, 0.67; $P = 0.016$).

p38

Phosphorylated p38 staining within the hippocampus did not differ from the pattern seen in control animals. Many cells were stained throughout the hippocampus bilaterally. The cellular morphological features were most consistent with glial staining, and neither the pyramidal cells nor the granule cells appeared to stain (*Fig. 3*).

Nissl Stain

Light microscopic analysis of cresyl violet sections did not reveal an abnormality, and no difference among hippocampi either within animals or between animals could be detected (*Fig. 3*).

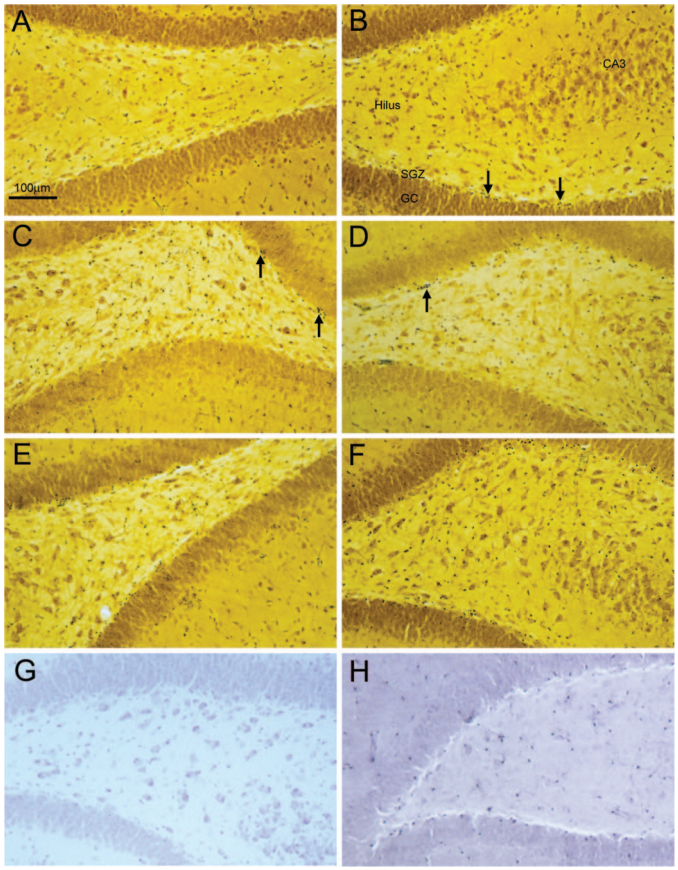

FIGURE 3. *Light microscopic photographs of rat hippocampal dentate gyrus stained for silver degeneration stain after 2 CGE* (A *and* B; *original magnification, ×50), 12 CGE* (C *and* D; *original magnification, ×50), and 60 CGE* (E *and* F; *original magnification, ×50) PBR and for cresyl violet* (G; *original magnification, ×50), and p38 MAPK* (H; *original magnification, ×50) after 60 CGE. Nontargeted sides* (A, C, *and* E) *and targeted sides* (B, D, *and* F) *of the same animal are demonstrated for silver stain. Targeted sides only are shown for cresyl violet and p38 MAPK. The dose dependency for the silver stain is best appreciated as one views the progression of staining on the nontargeted sides* (A, C, *and* E) *with incremental dosing, most likely the result of irradiation scatter.* Arrows *point to clusters of silver-stained cells (appearing* black). *Cresyl violet and p38 staining (punctate scattered nonneuronal cells appearing* dark purple) *appeared no different from controls in all animals studied.* GC, *granule cell layer;* SGZ, *subgranular proliferative zone;* CA3, *pyramidal layer CA3 of Ammon's horn.*

DISCUSSION

The main findings of our study are that 5 hours after low and clinically relevant doses of proton beam irradiation, DNAF, silver stain degeneration, and P-Erk1/2 are increased within the SGZ of the rat hippocampus, phosphorylated p38 is not, and colocalization of DNAF and P-Erk1/2 is incomplete. These findings extend our understanding of cellular responses and cell death patterns after irradiation in vivo.

TABLE 1. Silver stain-, deoxyribonucleic acid fragmentation-, and phospho-Erk1/2-positive cells per group of animals treated with different doses of hippocampal irradiation[a]

Group and side	Mean ± SD				Double as % DNAF	Double as % p-Erk1/2
	Silver stain	DNAF	p-Erk1/2	Double		
Control						
NT	0.2 ± 0.2	3.8 ± 0.8	0.5 ± 0.9	0.0 ± 0.0	0%	0%
T	0.3 ± 0.1	4.0 ± 2.5	3.0 ± 1.8	0.0 ± 0.0	0%	0%
2 CGE						
NT	1.5 ± 1.1	3.7 ± 3.3	5.8 ± 4.8	0.9 ± 0.7	27%	16%
T	31.3 ± 25.3	28.1 ± 9.8[b]	12.1 ± 5.2	5.9 ± 2.2	22%	49%
12 CGE						
NT	12.3 ± 11.7	11.7 ± 7.8	6.6 ± 3.2	1.9 ± 0.7	15%	29%
T	51.2 ± 38.1	46.3 ± 7.7[c,e]	35.3 ± 4.5[c,e]	14.3 ± 1.9	30%	40%
60 CGE						
NT	33.8 ± 26.7[d]	18.8 ± 13.0[d]	16.2 ± 4.9[e]	5.3 ± 3.4	28%	34%
T	79.1 ± 33.7[e]	37.6 ± 19.2[b,e]	33.2 ± 8.9[b,e]	16.2 ± 5.7	42%	49%

[a] Mean, mean number positive cells in the subgranular proliferative zone per tissue section for all animals in each dosage group; SD, standard deviation; DNAF, deoxyribonucleic acid fragmentation; p-Erk1/2, phospho-Erk1/2; Double as % DNAF, percentage of DNAF-positive cells that are also P-Erk1/2-positive; Double as % p-Erk1/2, percentage of P-Erk1/2-positive cells that are also DNAF-positive; NT, nontargeted; T, targeted; 2 CGE, cobalt-2 Gray equivalents; 12 CGE, cobalt-12 Gray equivalents; 60 CGE, cobalt-60 Gray equivalents.
[b] $P \leq 0.05$ for side-to-side differences when compared with side-to-side differences in controls.
[c] $P \leq 0.001$ for side-to-side differences when compared with side-to-side differences in controls.
[d] $P \leq 0.05$ for same-side comparisons to control group.
[e] $P \leq 0.001$ for same-side comparisons to control group.

Cell Death Hyperacutely after PBR

This study confirms prior findings of cell death after irradiation of cell cultured neurons (25, 31, 41) and after whole brain irradiation of fetal (3, 15, 21, 23, 29) and adult (1, 39, 44) rodents. The PBR model has several advantages over systemic or whole brain irradiation models and cell culture systems. The effects of irradiation on the intact animal brain permit analysis of alterations of specific subgroups of cells and regions within the hippocampus, which is not possible using cell cultures. Selective hippocampal irradiation permits assessment of neurophysiology and behavior after creation of a well-defined lesion. Because PBR delivers irradiation to a highly focused field, the nontargeted hippocampus may serve as an internal control, although our finding of modest contralateral changes emphasizes the importance of monitoring irradiation scatter. Cell death after irradiation is likely to be apoptotic. A review of the literature on apoptosis after irradiation reveals several common findings. First, apoptotic cell death can be demonstrated after very low doses of irradiation. Doses as low as 0.5 Gy, for example, lead to apoptotic cell death in the brain of young adult rats after whole brain irradiation, with the peak apoptotic labeling index found at 2 Gy (39). Others have found evidence for neuronal apoptosis at doses of 3 to 30 Gy in cell culture (25, 31, 41), at doses of 0.04 to 24 Gy in fetal or developing rodent brain (3, 13–16, 21, 23, 29, 35), and at doses of 5 to 30 Gy in adult rat brain (1, 39). Second, apoptosis within the nervous system seems to be restricted to the subependyma, the corpus callosum, and the SGZ. This presumably reflects the fact that cells with increased mitotic indices are more likely to be killed by irradiation. Last, apoptosis after irradiation is time-dependent. In irradiation studies on adult rat brain, for example, apoptosis was identified as early as 3 hours after irradiation and was completely absent by 48 hours (1, 39, 44).

Interestingly, apoptotic cell death has been confirmed in neoplastic tissue obtained from humans at long intervals after radiosurgery. Apoptosis was found after gamma knife radiosurgery in two cases of pituitary adenomas and in one case of an acoustic schwannoma resected 18 months after gamma knife radiosurgery (17). Apoptotic cell death, a form of programmed or active cell death, requires protein synthesis and is characterized by intranucleosomal DNA cleavage yielding approximately 200 base pair fragments, chromatin condensation, and fragmentation of nuclear material into apoptotic bodies. Although the gold standard for demonstrating occurrence of apoptosis has been the demonstration of apoptotic bodies using electron microscopy, the demonstration of DNAF using the TUNEL stain to label ends of fragmented DNA resulting from TUNEL biotin-labeled nick sites has been considered a useful surrogate marker for the occurrence of apoptosis. Several studies of irradiation-induced apoptosis have shown that this staining technique correlates well with apoptotic cell death as confirmed by oligonucleotide DNA laddering (14, 35) and blockade by cycloheximide (a protein synthesis inhibitor) (15, 44). One study demonstrated evidence for apoptosis using electron microscopy after irradiation but did not correlate this with a DNAF stain (21). Our laboratory uses the TUNEL stain as a technically simple, readily quantifiable method of analyzing DNAF in brain sections most likely representative of apoptotic cell death. The finding of silver staining of degenerating neurons, also restricted to the SGZ, suggests that at these cells have been killed by irradiation and are not simply staining for DNAF because of injurious DNA cleavage that may proceed to DNA repair with eventual cell survival. Differences in quantitative staining between silver stain and DNAF suggest that there may be some component of necrotic as well as apoptotic

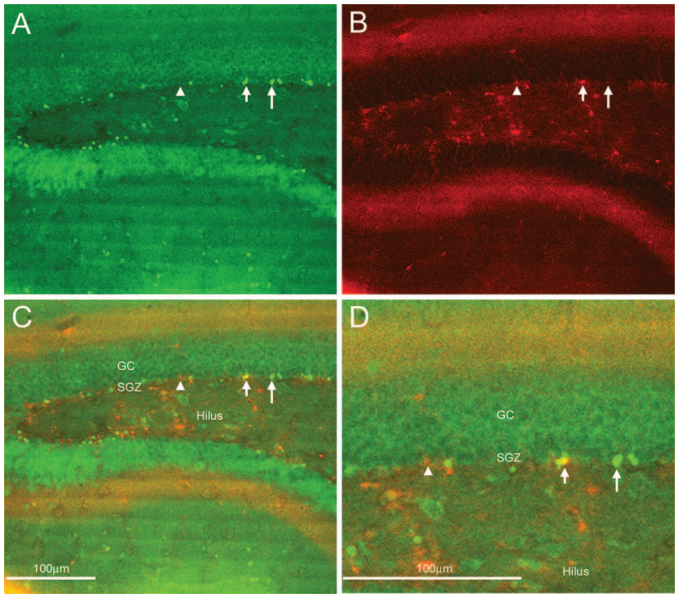

FIGURE 4. *Confocal microscopic identification of double-stained cells in the SGZ of rat hippocampal dentate gyrus after 12 CGE irradiation. Double staining of a given cell was determined by examining the specimen using single-channel microscopy (*A, *green channel;* B, *red channel; original magnification, ×50) as well as dual channel (*C: *original magnification, ×50; and* D: *original magnification, ×100) We used* arrows *and* arrowheads *to identify certain cells in the SGZ that are detected using the green channel only indicating DNAF staining only (*A *and* B, long arrow*), or using the red channel only indicating P-Erk1/2 staining only (*A *and* B, arrowhead*). When both channels of the confocal microscope are used, all cells are visible, with the DNAF only cells still staining green, the P-Erk1/2 only cells staining orange, and double-stained cells staining yellow (*C *and* D*). All* arrows *and* arrowheads *point to the same cells in all four figures.* GC, *granule cell layer;* SGZ, *subgranular proliferative zone.*

death, as is found in other animal experiments after stresses to the central nervous system (40).

P-Erk1/2 and Phosphorylated p38 Up-regulation Hyperacutely after PBR

Evolutionarily, MAPKs are thought to respond to mitogens that trigger transcription of early genes, thereby assisting mammalian cells to grow, proliferate, and survive (2, 20). The up-regulation of activated MAPK seems to be a sensitive marker to stress and has been demonstrated after administration of neurotrophins (10) or neurotransmitters (30) and in response to ischemia (6) and seizures (19).

Studies of MAPK activation in response to irradiation have been restricted to in vitro systems. MAPK activation after irradiation occurs in the hyperacute period and in response to low doses. Ionizing irradiation, for example, leads to the up-regulation of activated MAPK in various neoplastic cell lines after 2 to 20 Gy within minutes to hours (2, 7, 8, 11, 20, 26–28, 42). Several of these studies (2, 7, 8, 11, 28) showed specific up-regulation of P-Erk1/2 and/or p38. Our findings in vivo correlate well with these findings in cell cultures in that the MAPK cascade was induced with low doses after short latency.

We found bilateral SGZ P-Erk1/2 up-regulation when using 60 CGE. Although it is possible that this was caused by synaptic commissural activity between hippocampi, we believe that it represents irradiation scatter. Although irradiation is targeted to the ipsilateral hippocampus, based on the dosimetry curves for this model, it is clear that irradiation is seen by sites well beyond the ipsilateral hippocampus. We calculated that the middle of the contralateral hilus receives approximately 2 CGE of irradiation when delivering 60 CGE to the ipsilateral hippocampus. It therefore seems that the minimum dose of irradiation required to up-regulate P-Erk1/2 is between 2 CGE and 12 CGE.

The sensitivity of a given MAPK to up-regulation after irradiation in response to a given dose, latency, or model system is best underscored by our negative results with p38. In cell culture work, the MAPK p38 has demonstrated significant activation after both ultraviolet A (28) and ultraviolet B (8) irradiation and to a lesser extent after ionizing irradiation (24). Interestingly, the report demonstrating p38 activation failed to show irradiation change in Erk1/2 activation (28). By irradiating in vivo, we are able to be more anatomically specific and to conclude that at least in the rat hippocampus at the doses and latency used, we could not detect increased p38 activity.

Double-staining DNAF and Erk1/2 Colocalization

Prior studies in vitro have demonstrated that apoptotic cell death is causally related to activation of the Erk1/2 cascade by blocking the activation of this cascade with synthetic blockers such as PD98059 and by showing resultant alterations in the amount of apoptotic cell death (2, 20, 42). We hypothesized that Erk1/2 activation correlates with apoptosis and attempted to answer this question by performing double-staining immunofluorescence for DNAF and P-Erk1/2 and then examining individual cells for colocalization. Furthermore, we asked whether alterations in dose administered altered the relationship of Erk1/2 activation to cell death. Two advantages of an in vivo model in answering this question, therefore, are that both DNAF and P-Erk1/2 can be detected within an individual cell and that this colocalization can be anatomically localized and quantitated.

Our experiment was designed to ascertain a correlation between the two stains, and not a causation. That is, demonstration of stain for both DNAF and P-Erk1/2 in a given cell does not prove that one caused or was even necessary for the other to be present also. Given what is known about these two markers, a strong correlation may suggest causation. We did not find a significant correlation of these two markers, indicating that at the time studied, Erk1/2 need not be activated for a cell to undergo apoptosis. It is possible, however, that a given apoptotic cell not colocalizing with P-Erk1/2 might have colocalized had an earlier, or later, time point been

assayed. What is exciting, however, is that numerous cells did colocalize the two stains. Future experiments in which Erk1/2 blockers, such as PD98059, are used in conjunction with PBR and double staining may provide in vivo evidence for the activation of Erk1/2 as a prerequisite step in irradiation-induced apoptotic cell death.

Significance of SGZ Localization

The SGZ, a recently defined one- to two-cell layer of immature progenitor granule cells located at the granule cell-hilar border, may have special importance in being the only currently identified neuronal cell group that undergoes continued neurogenesis into adult life in both animals and humans (12, 36–38). The function of these cells is not known, but they may play a role in epileptogenesis because these cells are up-regulated in an animal seizure model. In that model, these newly born cells were shown to become mature granule cells with aberrant synaptic connections that may contribute to epileptogenicity (38).

Gamma knife irradiation recently was shown to reduce seizures in both an animal model and in humans in a small series (33, 43). A proposed mechanism consistent with this report would be that radiosurgery killed off hyperexcitable SGZ cells. The fact that seizures are the most common complication in humans in the acute period after radiosurgery also suggests that SGZ cells may be involved with maintenance of normal hippocampal electrophysiology (9). A role for SGZ cells in cognition also has been speculated. It has been hypothesized that SGZ cell death in response to irradiation may explain chronic neurobehavioral deficits found after cranial irradiation in humans (9). Understanding the role of SGZ cells and how we can manipulate their intracellular signals and ultimately their survival therefore may be very important. This model of early time-point analysis after PBR, possibly combined with the MAPK cascade blockers such as PD09859, may be one way to explore this.

CONCLUSION

We used a model of stereotactic PBR in the rat to demonstrate both metabolic changes and apoptotic cell death after low and clinically relevant doses in the hyperacute period. Targeting was restricted to one hippocampus, and all cellular alterations were restricted to the subgranular proliferative zone. Intracellular activation of the Erk1/2 MAPK signaling cascade was maximal at 12 CGE, whereas DNAF staining for apoptotic cell death and silver degeneration staining were elicited at 2 CGE and 60 CGE, respectively. Double-staining for DNAF and the Erk1/2 MAPK cascade was incomplete, suggesting that at 5 hours after irradiation, Erk1/2 activation is not sufficient to cause apoptotic cell death.

REFERENCES

1. Bellinzona M, Gobbel GT, Shinohara C, Fike JR: Apoptosis is induced in the subependyma of young adult rats by ionizing irradiation. **Neurosci Lett** 208:163–166, 1996.
2. Bonner JA, Vroman BT, Christianson TJ, Karnitz LM: Ionizing radiation-induced MEK and Erk activation does not enhance survival of irradiated human squamous carcinoma cells. **Int J Radiat Oncol Biol Phys** 42:921–925, 1998.
3. Borovitskaya AE, Evtushenko VI, Sabol SL: Gamma-radiation-induced cell death in the fetal rat brain possesses molecular characteristics of apoptosis and is associated with specific messenger RNA elevations. **Brain Res Mol Brain Res** 35:19–30, 1996.
4. Brisman JL, Cole AJ, Cosgrove GR, Thornton AF, Rabinov J, Bussiere M, Bradley-Moore M, Hedley-Whyte T, Chapman PH: Radiosurgery of the rat hippocampus: Magnetic resonance imaging, neurophysiological, histological, and behavioral studies. **Neurosurgery** 53:951–961, 2003.
5. Brisman JL, Cosgrove GR, Cole AJ: Phosphorylation of P42/P44 MAP kinase and DNA fragmentation in the rat perforant pathway stimulation model of limbic epilepsy. **Brain Res** 933:50–59, 2002.
6. Campos-Gonzalez R, Kindy MS: Tyrosine phosphorylation of microtubule-associated protein kinase after transient ischemia in the gerbil brain. **J Neurochem** 59:1955–1958, 1992.
7. Carter S, Auer KL, Reardon DB, Birrer M, Fisher PB, Valerie K, Schmidt-Ullrich R, Mikkelsen R, Dent P: Inhibition of the mitogen activated protein (MAP) kinase cascade potentiates cell killing by low dose ionizing radiation in A431 human squamous carcinoma cells. **Oncogene** 16:2787–2796, 1998.
8. Chen W, Bowden GT: Activation of p38 MAP kinase and ERK are required for ultraviolet-B induced c-fos gene expression in human keratinocytes. **Oncogene** 18:7469–7476, 1999.
9. Chin LS, Lazio BE, Biggins T, Amin P: Acute complications following gamma knife radiosurgery are rare. **Surg Neurol** 53:498–502, 2000.
10. Creuzet C, Loeb J, Barbin G: Fibroblast growth factors stimulate protein tyrosine phosphorylation and mitogen-activated protein kinase activity in primary cultures of hippocampal neurons. **J Neurochem** 64:1541–1547, 1995.
11. Dent P, Reardon DB, Park JS, Bowers G, Logsdon C, Valerie K, Schmidt-Ullrich R: Radiation-induced release of transforming growth factor alpha activates the epidermal growth factor receptor and mitogen-activated protein kinase pathway in carcinoma cells, leading to increased proliferation and protection from radiation-induced cell death. **Mol Biol Cell** 10:2493–2506, 1999.
12. Eriksson PS, Perfilieva E, Bjork-Eriksson T, Alborn AM, Nordborg C, Peterson DA, Gage FH: Neurogenesis in the adult human hippocampus. **Nat Med** 4:1313–1317, 1998.
13. Ferrer I: The effect of cycloheximide on natural and x-ray-induced cell death in the developing cerebral cortex. **Brain Res** 588:351–357, 1992.
14. Ferrer I, Macaya A, Blanco R, Olive M, Cinos C, Munell F, Planas AM: Evidence of internucleosomal DNA fragmentation and identification of dying cells in x-ray-induced cell death in the developing brain. **Int J Dev Neurosci** 13:21–28, 1995.
15. Ferrer I, Olive M, Ribera J, Planas AM: Naturally occurring (programmed) and radiation-induced apoptosis are associated with selective c-Jun expression in the developing rat brain. **Eur J Neurosci** 8:1286–1298, 1996.
16. Ferrer I, Serrano T, Alcantara S, Tortosa A, Graus F: X-ray-induced cell death in the developing hippocampal complex involves neurons and requires protein synthesis. **J Neuropathol Exp Neurol** 52:370–378, 1993.
17. Fukuoka S, Oka K, Seo Y, Tokanoshi M, Sumi Y, Nakamura H, Nakamura J, Ikawa F: Apoptosis following gamma knife radiosurgery in a case of acoustic schwannoma. **Stereotact Funct Neurosurg** 70[Suppl 1]:88–94, 1998.
18. Gallyas F, Wolff JR, Bottcher H, Zaborszky L: A reliable and sensitive method to localize terminal degeneration and lysosomes in the central nervous system. **Stain Technol** 55:299–306, 1980.
19. Gass P, Kiessling M, Bading H: Regionally selective stimulation of mitogen activated protein (MAP) kinase tyrosine phosphorylation after generalized seizures in the rat brain. **Neurosci Lett** 162:39–42, 1993.
20. Hagan M, Wang L, Hanley JR, Park JS, Dent P: Ionizing radiation-induced mitogen-activated protein (MAP) kinase activation in DU145 prostate carcinoma cells: MAP kinase inhibition enhances radiation-induced cell killing and G_2/M-phase arrest. **Radiat Res** 153:371–383, 2000.
21. Harmon BV, Allan DJ: X-ray-induced cell death by apoptosis in the immature rat cerebellum. **Scanning Microsc** 2:561–568, 1988.
22. Inoue O, Kobayashi K, Takai N, Furusawa Y, Ando K, Nakano T, Nishimura T: An increase in [^{3}H]QNB binding by proton-beam irradiation in intact rat brain: An apparent positive cooperativity of binding. **Neurosci Lett** 250:33–36, 1998.

23. Inouye M, Tamaru M, Kameyama Y: Effects of cycloheximide and actinomycin D on radiation-induced apoptotic cell death in the developing mouse cerebellum. **Int J Radiat Biol** 61:669–674, 1992.
24. Johnson NL, Gardner AM, Diener KM, Lange-Carter CA, Gleavy J, Jarpe MB, Minden A, Karin M, Zon LI, Johnson GL: Signal transduction pathways regulated by mitogen-activated/extracellular response kinase kinase kinase induce cell death. **J Biol Chem** 271:3229–3237, 1996.
25. Johnson MD, Xiang H, London S, Kinoshita Y, Knudson M, Mayberg M, Korsmeyer SJ, Morrison RS: Evidence for involvement of Bax and p53, but not caspases, in radiation-induced cell death of cultured postnatal hippocampal neurons. **J Neurosci Res** 54:721–733, 1998.
26. Kavanagh BD, Dent P, Schmidt-Ullrich RK, Chen P, Mikkelsen RB: Calcium-dependent stimulation of mitogen-activated protein kinase activity in A431 cells by low doses of ionizing radiation. **Radiat Res** 149:579–587, 1998.
27. Kharbanda S, Saleem A, Emoto Y, Stone R, Rapp U, Kufe D: Activation of Raf-1 and mitogen-activated protein kinases during monocytic differentiation of human myeloid leukemia cells. **J Biol Chem** 269:872–878, 1994.
28. Klotz LO, Pellieux C, Briviba K, Pierlot C, Aubry JM, Sies H: Mitogen-activated protein kinase (p38-, JNK-, ERK-) activation pattern induced by extracellular and intracellular singlet oxygen and UVA. **Eur J Biochem** 260:917–922, 1999.
29. Kubota Y, Takahashi S, Sun XZ, Sato H, Aizawa S, Yoshida K: Radiation-induced tissue abnormalities in fetal brain are related to apoptosis immediately after irradiation. **Int J Radiat Biol** 76:649–659, 2000.
30. Kurino M, Fukunaga K, Ushio Y, Miyamoto E: Activation of mitogen-activated protein kinase in cultured rat hippocampal neurons by stimulation of glutamate receptors. **J Neurochem** 65:1282–1289, 1995.
31. Manome Y, Datta R, Taneja N, Shafman T, Bump E, Hass R, Weichselbaum R, Kufe D: Coinduction of c-jun gene expression and internucleosomal DNA fragmentation by ionizing radiation. **Biochemistry** 32:10607–10613, 1993.
32. Martin C, Rubio I, Fatome M: Early and transient effects of neutron irradiation on dopamine receptors in the adult rat brain. **Neurosci Lett** 155:77–80, 1993.
33. Mori Y, Kondziolka D, Balzer J, Fellows W, Flickinger JC, Lunsford LD, Thulborn KR: Effects of stereotactic radiosurgery on an animal model of hippocampal epilepsy. **Neurosurgery** 46:157–165, 2000.
34. Nadler JV, Evenson DA: Use of excitatory amino acids to make axon-sparing lesions of hypothalamus. **Methods Enzymol** 103:393–400, 1983.
35. Nagai R, Tsunoda S, Hori Y, Asada H: Selective vulnerability to radiation in the hippocampal dentate granule cells. **Surg Neurol** 53:503–506, 2000.
36. Nakagawa E, Aimi Y, Yasuhara O, Tooyama I, Shimada M, McGeer PL, Kimura H: Enhancement of progenitor cell division in the dentate gyrus triggered by initial limbic seizures in rat models of epilepsy. **Epilepsia** 41:10–18, 2000.
37. Parent JM, Tada E, Fike JR, Lowenstein DH: Inhibition of dentate granule cell neurogenesis with brain irradiation does not prevent seizure-induced mossy fiber synaptic reorganization in the rat. **J Neurosci** 19:4508–4519, 1999.
38. Parent JM, Yu TW, Leibowitz RT, Geschwind DH, Sloviter RS, Lowenstein DH: Dentate granule cell neurogenesis is increased by seizures and contributes to aberrant network reorganization in the adult rat hippocampus. **J Neurosci** 17:3727–3738, 1997.
39. Peissner W, Kocher M, Treuer H, Gillardon F: Ionizing radiation-induced apoptosis of proliferating stem cells in the dentate gyrus of the adult rat hippocampus. **Brain Res Mol Brain Res** 71:61–68, 1999.
40. Portera-Cailliau C, Price DL, Martin LJ: Excitotoxic neuronal death in the immature brain is an apoptosis-necrosis morphological continuum. **J Comp Neurol** 378:70–87, 1997.
41. Radford IR, Murphy TK: Radiation response of mouse lymphoid and myeloid cell lines: Part III—Different signals can lead to apoptosis and may influence sensitivity to killing by DNA double-strand breakage. **Int J Radiat Biol** 65:229–239, 1994.
42. Reardon DB, Contessa JN, Mikkelsen RB, Valerie K, Amir C, Dent P, Schmidt-Ullrich RK: Dominant negative EGFR-CD533 and inhibition of MAPK modify JNK1 activation and enhance radiation toxicity of human mammary carcinoma cells. **Oncogene** 18:4756–4766, 1999.
43. Régis J, Bartolomei F, Rey M, Genton P, Dravet C, Semah F, Gastaut JL, Chauvel P, Peragut JC: Gamma knife surgery for mesial temporal lobe epilepsy. **Epilepsia** 40:1551–1556, 1999.
44. Shinohara C, Gobbel GT, Lamborn KR, Tada E, Fike JR: Apoptosis in the subependyma of young adult rats after single and fractionated doses of X-rays. **Cancer Res** 57:2694–2702, 1997.
45. Weiss S, Cataltepe O, Cole AJ: Anatomical studies of DNA fragmentation in rat brain after systemic kainate administration. **Neuroscience** 74:541–551, 1996.
46. Yang T, Wu SL, Liang JC, Rao ZR, Ju G: Time-dependent astroglial changes after gamma knife radiosurgery in the rat forebrain. **Neurosurgery** 47:407–415, 2000.

Acknowledgments

We thank Marc Bussiere, M.Sc., for irradiation planning and technique, Marek Ancukiewicz for assistance with statistical analysis, and Paul Chapman, M.D., and Jay S. Loeffler, M.D., for critical review of the manuscript. This study was supported by a fellowship grant from the Center for Innovative Minimally Invasive Therapy (JLB) and Grant NS036224 from the National Institute of Neurological Disorders and Stroke (AJC).

COMMENTS

Stereotactic radiosurgery constitutes a promising alternative to invasive neurosurgery, especially in cases of epilepsy. Despite its positive outcome to treat some forms of epilepsy, as well as some other 'functional diseases,' its use is limited by the fact that there is usually an important delay (>12 mo) between the intervention and the therapeutic effect. Such delayed response is reminiscent of what has been described in several types of epilepsy. There can be a long time interval between an initial insult and the appearance of epilepsy. It is thought that complex plastic modifications are triggered by the initial insult in neuronal networks and that these reorganizations, which are continuous, ultimately lead to the occurrence of seizures. Does the delayed response following radiosurgery follow a scheme similar (i.e., continuous reactive plasticity) to epilepsy?

The first step is to demonstrate that radiosurgery induces an early response in the system. In this article, Brisman et al. provide an answer to this issue, looking at the early consequence of proton beam irradiation of the hippocampus. Using a marker for cell death, they report on neuronal loss in the subgranular proliferative zone of the ipsilateral hippocampus. This region is particularly important, as it is a continuous source of dentate gyrus granule cells throughout life. Interestingly, neurogenesis in the dentate gyrus is increased after status epilepticus and the process is hypothesized to play a role in epileptogenesis and/or ictogenesis. Therefore, opposite processes are triggered: status epilepticus &U279E; neurogenesis &U279E; epilepsy (although this last causal relationship is far from established) and irradiation &U279E; loss of neuronal progenitors &U279E; antiepileptic. Although appealing, this simple (and simplistic) proposal is worth considering for future studies. Albeit less important, Brisman et al. also found cell death in the contralateral (nonirradiated) hippocampus, suggesting that some type of signal has been transmitted to the contralateral side. The other feature analyzed by Brisman et al. was the phosphorylation level of the two extracellular signal-regulated kinase (ERK). ERK is involved in numerous processes, including cell division and differentiation, as well as various forms of plasticity. ERK can regulate protein synthesis and function. Following irradiation, activated ERK levels were increased in both hippocampi (with a larger increase in the ipsilateral side). This seems to be a clear

indication that plastic modifications are triggered following irradiation. Increased levels of activated ERK are also found after status epilepticus. Although cell death and increased levels of activated ERK are not necessarily associated, both phenomena could constitute one early response of the system to irradiation, arguably leading to more complex reorganizations. It remains to be determined which plastic reorganizations are triggered by the activated ERK.

Jean Régis
Christophe Bernard
Marseille, France

The authors studied the immediate early effects of radiosurgery on the rat hippocampus at doses below, at, and above those commonly used in human tumor or vascular malformation radiosurgery. They were able to measure these effects (even at the lowest doses) and postulate on how radiosurgery to an epileptic focus or lesion may work. The concept of hyperacute radiation effects is not new and has been studied in numerous models. We previously completed a study of the early apoptosis response to radiosurgery (1) in vivo using a rat glioma model. It is my hope that this line of investigation will provide insight into avenues for radioprotection that we can deliver at the time of radiosurgery. Previous work with the 21-aminosteroid U-74389G showed evidence of brain protection without tumor protection in a rat glioma model (2).

Douglas Kondziolka
Pittsburgh, Pennsylvania

1. Witham T, Kondziolka D, Niranjan A, Fellows W, Chambers W: The characterization of tumor apoptosis after experimental radiosurgery. **Stereotact Funct Neurosurg** (in press).
2. Kondziolka D, Mori Y, Martinez AJ, McLaughlin M, Flickinger JC, Lunsford LD. Beneficial effects of the radioprotectant 21-aminosteroid U-74389G in a radiosurgery rat malignant glioma model. **Int J Radiat Oncol Biol Phys** 44:179–184, 1999.

To date, the vast majority of basic radiobiologic investigation has focused on the effects of fractionated irradiation. Unlike the slowly evolving benefits which accrue with standard radiotherapy, largely thought to be mediated through chromosomal damage, cell injury and death after radiosurgery is often best explained by epigenetic, nonchromosomal pathways. This premise stems from the fact that the effects of radiosurgery, both good and bad, can appear within hours of treatment, as seen in some patients with trigeminal neuralgia and at risk of post radiosurgical seizures. Given a somewhat unique mechanism of action, it is important to directly explore the basic science underlying radiosurgery and the hyperacute effects of large dose irradiation. Because no significant change is acutely observed on standard microscopy, the current immunohistochemical observations in Brisman et al.'s animal model have particular value. I encourage the authors to expand their promising line of experimentation to nonhippocampal regions of the rat brain in the future.

John R. Adler, Jr.
Stanford, California

In-training Liaison

The Congress of Neurological Surgeons exists for the purpose of promoting public welfare through the advancement of neurosurgery by a commitment to excellence in education and by a dedication to research and scientific knowledge.

—Mission Statement, Congress of Neurological Surgeons

Inherent in this commitment is a critical charge to serve the needs of the in-training individual. Considering the importance of this vital group within the neurosurgical community, the Journal has established a position within its board structure termed *In-training Liaison*. The individual holding this position will act as a spokesperson especially addressing the needs and concerns of individuals in in-training positions globally, as they relate to journal content and perspective.

The current individual holding this position is:

John S. Kuo, M.D., Ph.D.

Issues attendant to in-training matters should be conveyed to Dr. John S. Kuo at the Department of Neurological Surgery, LAC/USC Medical Center, 1200 N. State Street, Suite 5046, Los Angeles, CA 90033. Tel: 323/226-7421; Fax: 323/226-7833; email: kuo5577@hotmail.com.